Inorg. Chem. **2005**, *44*, 3569–3578

Influence of Steric and Electronic Properties of the Defect Site, Lanthanide Ionic Radii, and Solution Conditions on the Composition of Lanthanide(III) α_1-$P_2W_{17}O_{61}^{10-}$ Polyoxometalates

Cheng Zhang, Robertha C. Howell, Qun-Hui Luo, Heidi L. Fieselmann, Louis J. Todaro, and Lynn C. Francesconi*

Department of Chemistry, Hunter College and the Graduate School of the City University of New York, New York, New York 10021

Received January 22, 2005

This study identifies the principles that govern the formation and stability of Ln complexes of the $(\alpha_1$-$P_2W_{17}O_{61})^{10-}$ isomer. The conditional stability constants for the stepwise formation equilibria, K_{1cond} and K_{2cond}, determined by ^{31}P NMR spectroscopy, show that the high log K_{1cond}/log K_{2cond} ratio predicts the stabilization of the 1:1 Ln/$(\alpha_1$-$P_2W_{17}O_{61})^{10-}$ species. The value of log K_{1cond} increases as the Ln series is traversed, consistent with the high charge/size requirement of the basic α_1 defect site. The conditional stability constants, K_2, are very low and are highly dependent on the countercations in the buffer. The source of the instability is understood from the crystal structures of the early–mid lanthanide analogues, where the close contact of the $(\alpha_1$-$P_2W_{17}O_{61})^{10-}$ units result in severe steric encumbrance. The electronic properties of the α_1 defect along with the lanthanide ionic radii and countercation composition are important parameters that need to be considered for a rational synthesis of lanthanide polyoxometalates.

Introduction

Polyoxometalates (POMs) are transition-metal oxide clusters that have the most applications in the area of heterogeneous acid and oxidation catalysis.[1−4] However, their unique properties, such as redox tunability, electron withdrawing properties, and their robust nature, are currently exploited in multidisciplinary approaches, which should result in new applications.[5−7]

The addition of lanthanides to POMs has recently experienced a renewed interest for the creation of luminescent and electrochromic materials. For example, 1:2 Ln/monovacant POMs, such as $Eu(SiW_{11}O_{39})_2^{13-}$ or $Eu(P_2W_{17}O_{61})_2^{17-}$, identified by Peacock and Weakley,[8] incorporated into thin films show weak luminescence upon exciting into the POM framework.[9−15] Excitation spectra of thin films prepared by layer-by-layer or sol−gel techniques suggest that energy transfer from the organic portion to Eu(III) results in luminescence.[16,17] The Eu Preyssler ion has been incorporated into films using layer-by-layer and sol−gel techniques and, indeed, retains its luminescence and photochromic properties.[18−20]

* Author to whom correspondence should be addressed. E-mail: lfrances@hunter.cuny.edu.

(1) Katsoulis, D. E. *Chem. Rev.* **1998**, *98*, 359−388.
(2) Mizuno, N.; Misono, M. *Chem. Rev.* **1998**, *98*, 199−217.
(3) Kozhevnikov, I. V. *Chem. Rev.* **1998**, *98*, 171−198.
(4) Mizuno, N. In *Polyoxometalate Chemistry: From Topology via Self-Assembly to Applications*; Pope, M. T., Muller, A., Eds.; Kluwer Academic Publishers: Dordrecht, The Netherlands, 2001; pp 335−345.
(5) Anderson, T. M.; Neiwert, W. A.; Kirk, M. L.; Piccoli, P. M. B.; Schultz, A. J.; Koetzle, T. F.; Musaev, D. G.; Morokuma, K.; Cao, R.; Hill, C. L. *Science* **2004**, *306*, 2074−2077.
(6) Weinstock, I. A.; Barbuzzi, E. M. G.; Wemple, M. W.; Cowan, J. J.; Reiner, R. S.; Sonnen, D. M.; Heintz, R. A.; Bond, J. S.; Hill, C. L. *Nature* **2001**, *414*, 191−195.
(7) Kim, W. B.; Voitl, T.; Rodriguez-Rivera, G. J.; Dumesic, J. A. *Science (Washington, D.C.)* **2004**, *305*, 1280−1283.
(8) Peacock, R. D.; Weakley, T. J. R. *J. Chem. Soc. A* **1971**, *A*, 1836−1839.
(9) Wang, J.; Wang, H. S.; Fu, L. S.; Liu, F. Y.; Zhang, H. J. *Thin Solid Films* **2002**, *414*, 256−261.
(10) Wang, J.; Liu, F.; Fu, L.; Zhang, H. *Mater. Lett.* **2002**, *56*, 300−304.
(11) Wang, Y.; Wang, X.; Hu, C.; Shi, C. *J. Mater. Chem.* **2002**, *12*, 703−707.
(12) Xu, L.; Zhang, H.; Wang, E.; Wu, A.; Li, Z. *Mater. Chem. Phys.* **2002**, *77*, 484−488.
(13) Wang, J.; Wang, Z.; Wang, H.; Liu, F.; Fu, F.; Zhang, H. *J. Alloys Compd.* **2004**, *376*, 68−72.
(14) Ma, H.; Peng, J.; Zhou, B.; Han, Z.; Feng, Y. *Appl. Surf. Sci.* **2004**, *233*, 14−19.
(15) Sousa, F. L.; Ferreira, A. C. A. S.; Ferreira, R. A. S.; Cavaleiro, A. M. V.; Carlos, L. D.; Nogueira, H. I. S.; Rocha, J.; Trindade, T. *J. Nanosci. Nanotechnol.* **2004**, *4*, 214−220.
(16) Ma, H.; Peng, J.; Han, Z.; Feng, Y.; Wang, E. *Thin Solid Films* **2004**, *446*, 161−166.
(17) Wang, Z.; Wang, J.; Zhang, H. *Mater. Chem. Phys.* **2004**, *87*, 44−48.

10.1021/ic050103o CCC: $30.25
Published on Web 04/14/2005

We have also incorporated $(H_2O)_4Eu$ α_1-$P_2W_{17}O_{61}^{7-}$ into mesoporous MCM-41 with retention of the luminescence, albeit low.[21] However, to achieve the high luminescence required for films, devices, and sensor applications, sensitization of the lanthanides will likely be required because the absorbance of lanthanides is inherently low. Therefore, to take advantage of the useful properties of POMs, mixed organic−inorganic hybrids where the organic moiety sensitizes the Ln luminescence will be required. To accomplish this, the 1:1 Ln/monovacant POM families will be useful wherein the solvent molecules can be replaced by organic sensitizing groups.

Although the 1:1 Ln/monovacant POM families have been identified,[15,22−25] equilibria with the 1:2 Ln/monovacant POMs render the stabilization of the useful 1:1 species very difficult. This is especially problematic when trying to produce organic soluble 1:1 species by metathesis reactions. The multiple coordination requirements of lanthanides and the multiequilibria of lanthanide ions in aqueous solution as well as the often multiple basic sites of lacunary POMs significantly impact the solution's composition. Also, subtle, but nevertheless important, parameters that influence solution and solid-state speciation are the electronic and structural properties of the POM defect, the lanthanide ionic radii, and the solution conditions (pH, countercations, aging, etc.). The specific objective of this study is to understand how these parameters impact the solution and solid-state speciation of a family of lanthanide POMs that have important potential applications for the development of new materials, catalysts, and reagents. This understanding will guide us in the preparation of organic−inorganic Ln POM hybrid materials in aqueous and organic conditions that should improve the luminescence properties when incorporated into films. Moreover, this study should impact other fields; the species isolated here will facilitate the identification of Lewis acidic Ln POMs that will interact with organic substrates for catalysis applications. Also, the principles uncovered in this study should facilitate the use of α_1-$P_2W_{17}O_{61}^{10-}$ POMs for the extraction of radiolanthanides and actinides and even, by means of the differential stability constants, the separation of neighboring radiolanthanides.[26−31]

The study reported here addresses the formation and stability of the Ln α_1-$P_2W_{17}O_{61}^{10-}$ POM family. The monovacant α_1-$P_2W_{17}O_{61}^{10-}$ isomer is derived from the Wells−Dawson anion, α-$P_2W_{18}O_{62}^{6-}$, where the vacancy is located in the "belt" region. The creation of a vacancy in the cap region results in the α_2-$P_2W_{17}O_{61}^{10-}$ isomer. The nonequivalence of the cap and belt positions impacts the chemical properties of the Wells−Dawson POM and α_1 and α_2 transition-metal-substituted products. For example, electron transfer properties are clearly different in the cap and belt tungsten regions. Added electrons are first introduced into the belt region of the Wells−Dawson ion.[32,33] Transition-metal cations substituted into the α_1 and α_2 positions clearly show differences in electrochemistry; specifically, transition-metal cations substituted into the α_1 position are more readily reduced than when substituted into the α_2 position.[34−37] This has been ascribed to the orientation of the PO_4^{3-} tetrahedron, positioning a basic oxygen atom near the α_1 site, thus, favoring stronger coupling of the heterometal with the W atoms in the belt and variations in the protonation events. Theoretical treatments are consistent with these findings; the lowest unoccupied molecular orbital in the frontier orbitals of α-$P_2W_{18}O_{62}^{6-}$ (a''_1) consists of 96% α_1 character.[38] These structural and electronic differences, coupled with the lanthanide ionic radii, also have a significant impact on the speciation and stability of lanthanide complexes in solution and in solid state.

In pursuing solid-state and solution structure and speciation studies, the 1:1 species $(H_2O)_4Lu(\alpha_1$-$P_2W_{17}O_{61})^{7-}$, which is a monomer in solid state and in solution,[39,40] and $[(H_2O)_4Ce(\alpha_1$-$P_2W_{17}O_{61})]_2^{14-}$, a self-associated species in solid state that dissociates into a monomer in aqueous solution,[23] have been isolated. Here, we try to understand how the structural and electronic features of the α_1-$P_2W_{17}O_{61}^{10-}$ isomer impact the speciation and stability of its Ln complexes and, thus, their synthetic potential. We are using the findings described here for the purpose of producing pure 1:1 Ln/POMs that should be useful precursors for ternary complexes wherein the solvent (water) molecules are replaced by organic ligands.

(18) Xu, L.; Zhang, H.; Wang, E.; Kurth, D. G.; Li, Z. *J. Mater. Chem.* **2002**, *12*, 654−657.
(19) Liu, S.; Kurth, D. G.; Mohwald, H.; Volkmer, D. *Adv. Mater. (Weinheim, Ger.)* **2002**, *14*, 225−228.
(20) Gao, G.; Xu, L.; Wang, W.; An, W.; Qiu, Y. *J. Mater. Chem.* **2004**, *14*, 2024−2029.
(21) Xu, W.; Luo, Q.; Wang, H.; Francesconi, L. C.; Stark, R. E.; Akins, D. L. *J. Phys. Chem. B.* **2003**, *107*, 497−501.
(22) Sadakane, M.; Dickman, M. H.; Pope, M. T. *Angew. Chem., Int. Ed.* **2000**, *39*, 2914−2916.
(23) Sadakane, M.; Dickman, M. H.; Pope, M. T. *Inorg. Chem.* **2001**, *40*, 2715−2719.
(24) Sadakane, M.; Ostuni, A.; Pope, M. T. *J. Chem. Soc., Dalton Trans.* **2002**, 63−67.
(25) Mialane, P.; Lisnard, L.; Mallard, A.; Marrot, J.; Antic-Fidancev, E.; Aschehoug, P.; Vivien, D.; Secheresse, F. *Inorg. Chem.* **2003**, *42*, 2102−2108.
(26) Milyukova, M. S.; Litvina, M. N.; Myasoedov, B. P. *Radiokhimiya* **1983**, *25*, 706−712.
(27) Milyukova, M. S.; Varezhkina, N. S.; Myasoedov, B. F. *J. Radioanal. Nucl. Chem.* **1986**, *105*, 249−256.
(28) Milyukova, M. S.; Varezhkina, N. S.; Myasoedov, B. F. *J. Radioanal. Nucl. Chem.* **1988**, *121*, 403−408.
(29) Milyukova, M. S.; Varezhkina, N. S.; Myasoedov, B. F. *Sov. Radiochem., Engl. Trans.* **1990**, *32*, 361−367.
(30) Shilov, V. P. *Radiokhimiya* **1980**, *22*, 727−732.
(31) Yusov, A. B.; Shilov, V. P. *Radiochemistry (Moscow)* **1999**, *41*, 1−23.
(32) Kozik, M.; Hammer, C. F.; Baker, L. C. W. *J. Am. Chem. Soc.* **1986**, *108*, 2748−2749.
(33) Kozik, M.; Baker, L. C. W. *J. Am. Chem. Soc.* **1990**, *112*, 7604−7611.
(34) Contant, R.; Abbessi, M.; Canny, J.; Belhouari, A.; Keita, B.; Nadjo, L. *Inorg. Chem.* **1997**, *36*, 4961−4967.
(35) Contant, R.; Richet, M.; Lu, Y. W.; Keita, B.; Nadjo, L. *Eur. J. Inorg. Chem.* **2002**.
(36) Keita, B.; Girard, F.; Nadjo, L.; Contant, R.; Canny, J.; Richet, M. *J. Electroanal. Chem.* **1999**, *478*, 76−82.
(37) Keita, B.; Levy, B.; Nadjo, L.; Contant, R. *New. J. Chem.* **2002**, *26*, 1314−1319.
(38) Lopez, X.; Bo, C.; Poblet, J. M. *J. Am. Chem. Soc.* **2002**, *124*, 12574−12582.
(39) Bartis, J.; Dankova, M.; Lessmann, J. J.; Luo, Q.-H.; Horrocks, W. D., Jr.; Francesconi, L. C. *Inorg. Chem.* **1999**, *38*, 1042−1053.
(40) Luo, Q.; Howell, R. C.; Dankova, M.; Bartis, J.; Williams, C. W.; Horrocks, W. D., Jr.; Young, J. V. G.; Rheingold, A. L.; Francesconi, L. C.; Antonio, M. R. *Inorg. Chem.* **2001**, *40*, 1894−1901.

Experimental Section

General. All of the reagents were commercially available and used without further purification. $K_{10}[\alpha_1\text{-}P_2W_{17}O_{61}]$ was prepared following the method of Contant (*Inorg. Synth.* **1990**, *27*, 71). Elemental analyses were carried out by inductive coupled plasma atomic emission spectrometry (Spectroflame M120E).

Synthesis and Crystallization of $[Ln(\alpha_1\text{-}P_2W_{17}O_{61})_2]^{17-}$ (Ln = La^{3+}, Eu^{3+}, Nd^{3+}, Dy^{3+}, Ho^{3+}, Er^{3+}). A prototypical reaction for lanthanum is given. $K_9Li[\alpha_1\text{-}P_2W_{17}O_{61}]$ (1 g, 0.20 mmol) was dissolved in 12 mL of buffer solution of LiOAc (0.285 M) at pH 4.75 at room temperature, and 0.115 mL of 0.90 M $LaCl_3$ solution (0.10 mmol) was added slowly to the above solution with vigorous stirring. The solution was stirred vigorously for 15 min, followed by the addition of KCl (0.32 g, 4.29 mmol). A white precipitate formed and was collected by filtration. The white solid was redissolved in a minimum amount of LiOAc buffer (0.285 M) pH 4.75 and, then, was placed in the freezer (4 °C). After 3 days, colorless rectangular crystals had formed.

Elemental Analyses Elem Anal. Calcd for $K_{14}(H_3O)_3[La(\alpha_1\text{-}P_2W_{17}O_{61})_2]\cdot 4KCl\cdot 64H_2O$: La, 1.23; W, 55.23; P, 1.09; K, 4.84. Found: La, 1.25; W, 57.29; P, 1.22; K, 4.84. Elem Anal. Calcd for $K_{14}(H_3O)_3[Eu(\alpha_1\text{-}P_2W_{17}O_{61})_2]\cdot 4KCl\cdot 64H_2O$: Eu, 1.34; W, 55.17; P, 1.09; K, 4.83. Found: Eu, 1.34; W, 55.19; P, 1.11; K, 4.80. Elem Anal. Calcd for $K_{14}(H_3O)_3[Nd(\alpha_1\text{-}P_2W_{17}O_{61})_2]\cdot 4KCl\cdot 64H_2O$: Nd, 1.37; W, 59.38; P, 1.18; K, 7.01. Found: Nd, 1.34; W, 58.04; P, 1.18; K, 6.53. Elem Anal. Calcd for $K_{14}(H_3O)_3[Dy(\alpha_1\text{-}P_2W_{17}O_{61})_2]\cdot 4KCl\cdot 64H_2O$: Dy, 1.54; W, 59.28; P, 1.17; K, 6.67. Found: Dy, 1.55; W, 59.77; P, 1.14; K, 6.65. Elem Anal. Calcd for $K_{14}(H_3O)_3[Ho(\alpha_1\text{-}P_2W_{17}O_{61})_2]\cdot 4KCl\cdot 64H_2O$: Ho, 1.56; W, 59.27; P, 1.17; K, 6.67. Found: Ho, 1.56; W, 59.03; P, 1.10; K, 6.65. Elem Anal. Calcd for $K_{14}(H_3O)_3[Er(\alpha_1\text{-}P_2W_{17}O_{61})_2]\cdot 4KCl\cdot 64H_2O$: Er, 1.58; W, 59.26; P, 1.17; K, 6.67. Found: Er, 1.55; W, 57.90; P, 1.17; K, 6.52. The crystals of $[Ln(\alpha_1\text{-}P_2W_{17}O_{61})_2]^{17-}$ (Ln = Eu^{3+}, Nd^{3+}, Dy^{3+}, Ho^{3+}, Er^{3+}) were grown in the same fashion. The crystal shapes are all similar except for the size and color. The Eu and Dy analogue crystals are colorless, the Nd analogue crystals are light blue, and the Ho and Er crystals are very light pink.

Elemental Analysis by ISP. (i) Standard Solution Preparation. The standard solutions of P (0.2, 0.4, 0.6, 0.8, 1.2 ppm), Eu (1, 2, 4, 6 ppm), La (1, 2, 4, 6 ppm), Nd (1, 2, 4, 6 ppm), Dy (1, 2, 4, 6 ppm), Ho (1, 2, 4, 6 ppm), Er (1, 2, 4, 6 ppm), W (20, 40, 60, 80, 120 ppm), and K (1, 3, 5, 7 ppm) was prepared by diluting a 1000 ppm ICP standard solution (GFS Chemicals, Inc.) with distilled water.

(ii) Sample Preparation. Crystals of $[Ln(\alpha_1\text{-}P_2W_{17}O_{61})_2]^{17-}$ (Ln = La^{3+}, Eu^{3+}, Nd^{3+}, Dy^{3+}, Ho^{3+}, Er^{3+}) were collected by filtration and were placed in uncovered, carefully labeled small vials, and then they were put into a desiccator ($CaSO_4$ as drying agent) vacuum for 1.5 h. The samples were left in the closed evacuated desiccator overnight. Afterward, 0.0148 g of $[Eu(\alpha_1\text{-}P_2W_{17}O_{61})_2]^{17-}$, 0.0106 g of $[La(\alpha_1\text{-}P_2W_{17}O_{61})_2]^{17-}$, 0.0277 g of $[Nd(\alpha_1\text{-}P_2W_{17}O_{61})_2]^{17-}$, 0.0264 g of $[Dy(\alpha_1\text{-}P_2W_{17}O_{61})_2]^{17-}$, 0.0294 g of $[Ho(\alpha_1\text{-}P_2W_{17}O_{61})_2]^{17-}$, and 0.0284 g of $[Er(\alpha_1\text{-}P_2W_{17}O_{61})_2]^{17-}$ were each dissolved in a 25 mL volumetric flask with distilled water. A total of 2 and 4 mL of the first two solutions and 1 and 2 mL of the latter four solutions from each flask were poured into individual 25 mL volumetric flasks to prepare the ICP samples.

(iii) Method. The maximum wavelengths for the different elements were selected (P, 213.618 nm; Eu, 381.970 nm; La, 379.478 nm; Nd, 406.109 nm; Dy, 353.170 nm; Ho, 345.600 nm; Er, 337.271 nm; W, 239.709 nm; K, 766.496 nm). A calibration curve for each element was constructed. After the calibration curve of each element was completed, the concentration (in ppm) was determined for two solutions of each sample {47.36 and 94.72 μg/mL of $[Eu(\alpha_1\text{-}P_2W_{17}O_{61})_2]^{17-}$, 33.96 and 67.84 μg/mL of $[La(\alpha_1\text{-}P_2W_{17}O_{61})_2]^{17-}$, 44.32 and 88.64 μg/mL of $[Nd(\alpha_1\text{-}P_2W_{17}O_{61})_2]^{17-}$, 42.24 and 84.48 μg/mL of $[Dy(\alpha_1\text{-}P_2W_{17}O_{61})_2]^{17-}$, 47.04 and 94.08 μg/mL of $[Ho(\alpha_1\text{-}P_2W_{17}O_{61})_2]^{17-}$, and 45.44 and 90.88 μg/mL of $[Er(\alpha_1\text{-}P_2W_{17}O_{61})_2]^{17-}$}. The concentrations in ppm were then converted to weight percents of each element.

Collection of NMR Data. All of the NMR spectra were recorded on a JEOL GX-400 spectrometer with 5 or 10 mm tubes. Resonance frequencies are 161.8 MHz for ^{31}P and 16.7 for ^{183}W. Chemical shifts are given with respect to external 85% H_3PO_4 for ^{31}P and 2.0 M Na_2WO_4 for ^{183}W. Typical acquisition parameters for ^{31}P spectra included the following: spectral width, 10 000 Hz; acquisition time, 0.8 s; pulse delay, 1 s; pulse width, 15 μs (50° tip angle). Anywhere from 200 to 1000 scans were required. For ^{183}W spectra, typical conditions included the following: spectral width, 10 000 Hz; acquisition time, 1.6 s; pulse delay, 0.5 s; pulse width, 50 μs (45° tip angle). Anywhere from 1000 to 30 000 scans were acquired. For all of the spectra, the temperature was controlled to 25 ± 0.2°. For ^{31}P and ^{183}W chemical shifts, the convention used is that the more negative chemical shifts denote upfield resonances.

Conditional Stability Constant Determination. (A) Determination of the Conditional K_1. (1) Sample Preparation. All of the lanthanides were standardized by EDTA (standard solution, Aldrich) with xylenol orange as an indicator. The molecular weight of the ligand $K_{10}[\alpha_1\text{-}P_2W_{17}O_{61}]$ was obtained by titrating $[\alpha_1\text{-}P_2W_{17}O_{61}]^{10-}$ with $CoCl_2$ (0.2979 M) (standardized by EDTA), monitoring by UV−vis (the absorbance was recorded at 544 nm). The procedure for the preparation of the ^{31}P NMR sample is as follows: 0.0425 g of $K_{10}[\alpha_1\text{-}P_2W_{17}O_{61}]$ was dissolved in 2 mL of lithium acetate buffer (pH = 4.75, 0.5 M, 20% D_2O), and 31.0 μL of $LnCl_3$ (0.2004 M) and 25 μL of EDTA (0.0974 M) were added. The solution was clear. After 8 h at room temperature, the solution reached its equilibrium. The ^{31}P NMR spectrum was recorded. An external standard, phosphoric acid (0.009−0.013 M), which was placed in a smaller tube inside of a 10-mm NMR tube, was used to quantitatively monitor the concentrations of $[\alpha_1\text{-}P_2W_{17}O_{61}]^{10-}$. At least four determinations were performed for each lanthanide. A sample ^{31}P NMR spectrum is shown in Figure 1a. The conditional K_1 equilibrium constants of $[Ln(\alpha_1\text{-}P_2W_{17}O_{61})_2]^{17-}$ are displayed in Table 1.

(2) Standard Curve Preparation and Use. The calibration curves of $[\alpha_1\text{-}P_2W_{17}O_{61}]^{10-}$ versus the standard (STD) were obtained by monitoring the ^{31}P NMR spectra of four concentrations, 0.5, 1.2, 2.0, and 3.0 mM, under the same conditions as for the above competition experiments. The intensity of $[\alpha_1\text{-}P_2W_{17}O_{61}]^{10-}$/STD plotted against the concentration of $[\alpha_1\text{-}P_2W_{17}O_{61}]^{10-}$ gives a straight line, which means the intensity of $[\alpha_1\text{-}P_2W_{17}O_{61}]^{10-}$ (the peak at −8.4 ppm, for example) I_L versus the intensity of STD I_{STD} is proportional to the concentration of $[\alpha_1\text{-}P_2W_{17}O_{61}]^{10-}$. $S_g = I_L/I_{STD} = \kappa[L]_t$; S_g is obtained from the ^{31}P NMR spectra. Thus, $[L]_t = S_g/\kappa$ can be used directly for the calculation of K_{eq}.

(B) Determination of the Conditional K_2. (1) Equilibrium Constant Measurement of $[Ln(\alpha_1\text{-}P_2W_{17}O_{61})_2]^{17-}$ (Ln = La^{3+}, Nd^{3+}, Eu^{3+}, Dy^{3+}, Ho^{3+}, Er^{3+}) with Different Countercations Monitored by ^{31}P NMR. The buffer solutions of LiOAc (0.02 M), NaOAc (0.02M), KOAc (0.02 M), and CsOAc (0.02 M) (30% D_2O) at pH 4.75 ± 0.10 were prepared. In a 10-mm NMR tube, 0.06 g of $(\alpha_1\text{-}P_2W_{17}O_{61})^{10-}$ was dissolved in 2 mL of each of the above buffer solutions, and then different Ln^{3+} {$[(\alpha_1\text{-}P_2W_{17}O_{61})^{10-}/Ln^{3+}$

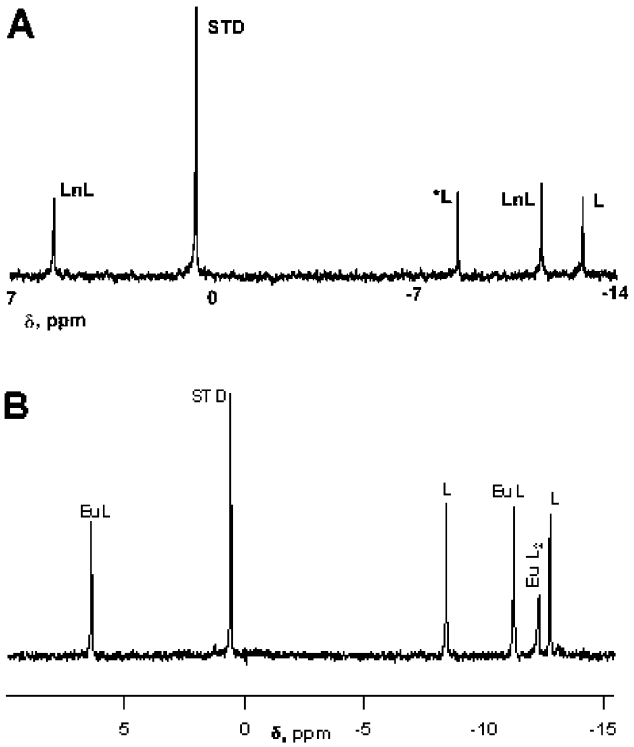

Figure 1. Examples of ^{31}P NMR spectra for conditional K_1 and K_2 constants. (A) Equilibrium solution of Eu^{3+}, $(\alpha_1\text{-}P_2W_{17}O_{61})^{10-}$, and competitive ligand EDTA at LiOAc (0.5 M) pH 4.75. STD = standard, LnL = $Eu(\alpha_1\text{-}P_2W_{17}O_{61})^{10-}$ (B) ^{31}P NMR spectrum of an equilibrium solution of Eu^{3+} and $(\alpha_1\text{-}P_2W_{17}O_{61})^{10-}$ in a 1:2 ratio at NaOAc (0.04 M) pH 4.75. STD is the external standard (0.01228 M of H_3PO_4 in H_2O), EuL is $[Eu(\alpha_1\text{-}P_2W_{17}O_{61})]^{7-}$, L is ligand $(\alpha_1\text{-}P_2W_{17}O_{61})^{10-}$, EuL_2 is $[Eu(\alpha_1\text{-}P_2W_{17}O_{61})_2]^{17-}$. Note: In spectrum B, we find that the downfield ^{31}P peak for EuL_2 (close to Eu) is broad and not easily observed, especially when in low concentration (see Figure S5 in the Supporting Information). The equilibrium expression is written in terms of the initial Eu concentration and the POM concentration (see the Data Analysis section), the concentrations are higher for these species, and the resonances are sharp and, thus, can be successfully integrated.

stoichiometric ratio = 2.2]} were added separately; the resulting solution was shaken for about 30 min and, then, was stored at room temperature for 5 h. The ^{31}P NMR spectra were recorded. The external standard was phosphoric acid (0.009−0.013 M) in a small tube, which was placed inside a 10-mm NMR tube. The calibration curves of $(\alpha_1\text{-}P_2W_{17}O_{61})^{10-}$ versus STD were obtained at four different concentrations, 0.5, 1.0, 2.0, and 3.0 mM, by monitoring the ^{31}P NMR spectra. The conditional K_2 equilibrium constants of $[Ln(\alpha_1\text{-}P_2W_{17}O_{61})_2]^{17-}$ at different countercations, Li^+, Na^+, K^+, and Cs^+, are displayed in Table 1. At least four determinations were performed for each analysis. A sample ^{31}P NMR spectrum is shown in Figure 1b.

(2) Sample Standard Curve. The calibration curve of $(\alpha_1\text{-}P_2W_{17}O_{61})^{10-}$ is the same as that in the determination of $K_{1\text{cond.}}$

Data Analysis. (A) Determination of Conditional Formation Constants, K_1, for Ln(III) α1 1:1 Complexes Obtained from Ligand−Ligand Competition Studies. Eq 1 represents the competitive equilibrium expression that was set up and solved. In this expression, Ln represents the lanthanide ion, L represents the $(\alpha_1\text{-}P_2W_{17}O_{61})^{10-}$ ligand, and L′ represents the competitive EDTA ligand.

$$\mathrm{LnL} + \mathrm{L}' \rightleftharpoons \mathrm{LnL}' + \mathrm{L} \qquad K_{\mathrm{eq}} \tag{1}$$

We can write the expression for the equilibrium constant (K_{eq}) for eq 1 in terms of the conditional equilibrium constants for EDTA (K' cond) and the conditional equilibrium constant for the 1:1 Ln $(\alpha_1\text{-}P_2W_{17}O_{61})^{10-}$ species, shown in eq 2.

$$K_{\mathrm{eq}} = \frac{[\mathrm{LnL}'][\mathrm{L}]_t}{[\mathrm{LnL}][\mathrm{L}']_t} = \frac{K'_{\mathrm{cond}}}{K_{1\mathrm{cond}}} = \frac{K'\alpha'_{\mathrm{L}}}{K_1\alpha_{\mathrm{L}}} \tag{2}$$

K_1 and K' are the thermodynamic formation constants corresponding to eqs 3 and 4, respectively.

$$\mathrm{Ln} + \mathrm{L} \rightleftharpoons \mathrm{LnL} \qquad K_1 \tag{3}$$

$$\mathrm{Ln} + \mathrm{L}' \rightleftharpoons \mathrm{LnL}' \qquad K' \tag{4}$$

K_{cond} is equal to eq 5:

$$K_{\mathrm{cond}} = \frac{[\mathrm{LnL}]}{[\mathrm{Ln}][\mathrm{L}]_t} = K\alpha_{\mathrm{L}} \tag{5}$$

$[L]_t$ is the sum of the equilibrium concentrations of the nonprotonated form and all of the protonated forms of ligand L.

$$[\mathrm{L}]_t = [\mathrm{L}^{n-}] + [\mathrm{HL}^{(n-1)-}] + [\mathrm{H_2L}^{(n-2)-}] + \cdots \tag{6}$$

$$\alpha_{\mathrm{L}} = \frac{[\mathrm{L}]}{[\mathrm{L}]_t} = \frac{1}{(1 + K_1^{\mathrm{H}}[\mathrm{H}] + K_1^{\mathrm{H}}K_2^{\mathrm{H}}[\mathrm{H}]^2 + \cdots)} \tag{7}$$

K_n^{H} is the nth protonation constant of L; an analogous expression applies for the competitive ligand, L′.

The mass balance equations for eq 1, where i indicates the initial concentration of the species, are

$$[\mathrm{Ln}]_i = [\mathrm{LnL}] + [\mathrm{LnL}'] \tag{8}$$

$$[\mathrm{L}]_i = [\mathrm{LnL}] + [\mathrm{L}]_t \tag{9}$$

$$[\mathrm{L}']_i = [\mathrm{LnL}'] + [\mathrm{L}']_t \tag{10}$$

When eqs 8, 9, and 10 are combined, the equilibrium expression for eq 1 is reduced to a function of $[L]_t$, and the initial concentrations.

$$K_{\mathrm{eq}} = \frac{([\mathrm{Ln}]_i - [\mathrm{L}]_i + [\mathrm{L}]_t)[\mathrm{L}]_t}{([\mathrm{L}]_i - [\mathrm{L}]_t)([\mathrm{L}']_i - [\mathrm{Ln}]_i + [\mathrm{L}]_i - [\mathrm{L}]_t)} \tag{11}$$

The intensity of the $[\alpha_1\text{-}P_2W_{17}O_{61}]^{10-}$ peak I_{L} at −8.4 ppm versus the intensity of the STD peak I_{STD} is proportional to the concentration of $[\alpha_1\text{-}P_2W_{17}O_{61}]^{10-}$.

$$S_{\mathrm{g}} = \frac{I_{\mathrm{L}}}{I_{\mathrm{STD}}} = \kappa[\mathrm{L}]_t \tag{12}$$

$$K_{\mathrm{eq}} = \frac{([\mathrm{Ln}]_i - [\mathrm{L}]_i + S_{\mathrm{g}}/\kappa)(S_{\mathrm{g}}/\kappa)}{([\mathrm{L}]_i - S_{\mathrm{g}}/\kappa)([\mathrm{L}']_i - [\mathrm{Ln}]_i + [\mathrm{L}]_i - S_{\mathrm{g}}/\kappa)} \tag{13}$$

Eq 13 can be reduced to the experimental integration data and the initial concentrations of L and L′, shown in eq 14.

$$K_{\mathrm{eq}} = \frac{(S_{\mathrm{g}}/\kappa)^2}{([\mathrm{L}]_i - S_{\mathrm{g}}/\kappa)([\mathrm{L}']_i - S_{\mathrm{g}}/\kappa)} \tag{14}$$

Once K_{eq} is obtained, $K_{1\mathrm{cond}}$ can be calculated from eq 2 because K'_{cond} is known. Table S1 in the Supporting Information shows the conditional stability constants of Ln EDTA complexes at pH 4.75.

Table 1. Conditional Stability Constants for Lanthanide Complexes of α_1-$P_2W_{17}O_{61}^{10-}$

lanthanide	La	Nd	Eu	Dy	Er	Yb	Lu
log K_1[a]	8.00 ± 0.17	8.63 ± 0.22	10.35 ± 0.22	11.08 ± 0.15	11.62 ± 0.09	12.21 ± 0.12	12.50 ± 0.09
log K_2 (Li^+)[b]	2.190 ± 0.017	2.069 ± 0.025	2.177 ± 0.003	2.132 ± 0.008	2.233 ± 0.006	1.874 ± 0.007	1.874 ± 0.007
logK_2 (Na^+)[b]	2.257 ± 0.03	2.559 ± 0.009	2.421 ± 0.022	2.493 ± 0.009	2.264 ± 0.021	2.043 ± 0.033	2.042 ± 0.008
log K_2 (K^+)[b]	2.609 ± 0.015	2.788 ± 0.005	2.785 ± 0.008	2.677 ± 0.018	2.351 ± 0.024	2.313 ± 0.054	2.139 ± 0.026
log K_2 (Cs^+)[b]	3.139 ± 0.026	3.321 ± 0.023	3.220 ± 0.041	3.099 ± 0.014	2.517 ± 0.006	2.521 ± 0.003	2.185 ± 0.006
log K_1/K_2[c]	3.65	4.17	4.75	5.19	5.20	5.98	6.67

[a] K_{1cond} determined from competition experiments, monitored by ^{31}P NMR, using EDTA as a competitive ligand. Conditions: pH = 4.75; 0.5 M $LiNO_3$; 25 °C. See text and Supporting Information for details. [b] K_{2cond} determined by ^{31}P NMR measurements, described in text and Supporting Information. Conditions: pH = 4.75; 0.02 M Macetate (M = Li, Na, K, Cs); 25 °C. [c] K_{2cond}: 0.02 M LiOAc.

Sample calculations to obtain K_{eq} and K_{1cond} are shown in the Supporting Information.

(B) Determination of Conditional Formation Constants, K_{2cond}, for Ln(III) α1 1:2 Complexes. The reaction of Eu with $[\alpha_1$-$P_2W_{17}O_{61}]^{10-}$ forms the 1:1 complex. Excess $[\alpha_1$-$P_2W_{17}O_{61}]^{10-}$ ligand sets up an equilibrium between the 1:1 and 1:2 complexes, as demonstrated in eq 15. We are assuming here that the 1:1 complex of LnL forms immediately, Ln + L → LnL, thus, there are no noncoordinated Ln ions present in the solution.

$$\mathrm{Ln} + \mathrm{L} \rightarrow \mathrm{LnL} + \mathrm{L} \rightleftharpoons \mathrm{LnL_2}\ K_{2cond} \tag{15}$$

The mass balance equations are shown in eqs 16 and 17, below.

$$[\mathrm{Ln}]_0 = [\mathrm{LnL}]_t + [\mathrm{LnL_2}]_t + [\mathrm{Ln}]_t \tag{16}$$

$$[\mathrm{L}]_0 = [\mathrm{LnL}]_t + [\mathrm{L}]_t + 2[\mathrm{LnL_2}]_t \tag{17}$$

Hence,

$$[\mathrm{LnL}]_t = [\mathrm{Ln}]_0 - [\mathrm{LnL_2}]_t \tag{18}$$

and

$$[\mathrm{LnL}]_t = [\mathrm{L}]_0 - [\mathrm{L}]_t - 2[\mathrm{LnL_2}]_t \tag{19}$$

therefore,

$$[\mathrm{Ln}]_0 - [\mathrm{LnL_2}]_t = [\mathrm{L}]_0 - [\mathrm{L}]_t - 2[\mathrm{LnL_2}]_t \tag{20}$$

$$[\mathrm{LnL_2}]_t = [\mathrm{L}]_0 - [\mathrm{L}]_t - [\mathrm{Ln}]_0 \tag{21}$$

$$[\mathrm{LnL}]_t = [\mathrm{L}]_t - [\mathrm{L}]_0 + 2[\mathrm{Ln}]_0 \tag{22}$$

$$K_{2cond} = \frac{[\mathrm{LnL_2}]_t}{[\mathrm{LnL}]_t[\mathrm{L}]_t} = \frac{[\mathrm{L}]_0 - [\mathrm{L}]_t - [\mathrm{Ln}]_0}{([\mathrm{L}]_t - [\mathrm{L}]_0 + 2[\mathrm{Ln}]_0)[\mathrm{L}]_t} \tag{23}$$

$[L]_t$ can be expressed in terms of S_g/κ, as for K_{1cond} above, and K_{2cond} can be calculated using S_g/κ and the initial concentrations. An example of the data analysis is shown in the Supporting Information.

Single-Crystal X-ray Structure Determination. Blocklike crystals of $[La(\alpha_1$-$P_2W_{17}O_{61})_2]^{17-}$ were isolated from the solution and examined under a thin layer of mineral oil using a polarizing microscope. A suitable crystal was chosen and mounted on a glass fiber while still coated in oil; the crystal was then immediately frozen to 100 K on a Bruker Nonius Kappa CCD diffractometer equipped with a sealed tube Mo anode (Kα radiation, λ = 0.71073 Å) and a graphite monochromator. Because crystals of $[Eu(\alpha_1$-$P_2W_{17}O_{61})_2]^{17-}$ turned dark or broke into pieces once out of the oil, the selected crystals were mounted in the loop to make sure the crystals stayed in the oil and then quickly placed in a stream of cold nitrogen. Data collection, indexing, and initial cell refinements were all handled using accompanying Nonius software. The SHELX package of software was used to solve and refine the restructures. The heaviest atoms were located by direct methods, and the remaining atoms were found in subsequent Fourier difference maps. Data for crystals of $K_{14}(H_3O)_3[Ln(\alpha_1$-$P_2W_{17}O_{61})_2]\cdot nH_2O$ (Ln = Nd^{3+}, Eu^{3+}, Er^{3+}) were collected using a cryoloop that was then frozen at 100 K. These crystals decomposed easily upon removal from the freezer and during the X-ray experiment. The crystal data and structure refinement data for the La(III) analogue are displayed in Table 2, and those for Nd(III) and Eu(III) are displayed in Table S2 in the Supporting Information. Selected bond lengths are displayed in Table 3. The X-ray crystal structure of the La derivative is shown in Figure 2.

Table 2. Crystal Data and Structure Refinement for $K_{14}(H_3O)_3[La(\alpha_1$-$P_2W_{17}O_{61})_2]\cdot nH_2O$

empirical formula	$K_{14}LaP_4W_{34}O_{158}$
formula weight	9589.09
crystal system	monoclinic
space group	*C*2/*c*
temp, K	100 K
wavelength, Å	0.71073
a, Å	41.339(8)
b, Å	15.636(3)
c, Å	24.988(5)
α, deg	90
β, deg	104.53(3)
γ, deg	90
vol, Å^3	15635(5)
Z	4
calcd density, g/cm^3	4.074
abs coeff, mm^{-1}	25.692
F (000)	16652
θ range, deg	1.40°−27.57°
limiting indices	−53 < h < 53, −20 < k < 20, −32 < l < 32
reflns collected/unique	34400/17934 [R(int) = 0.0557]
refinement meth	full-matrix least squares on F^2
data/restraints/parameters	17934/0/568
GOF on F^2	1.070
final R indices [$I > 2\sigma(I)$]	R1 = 0.0744, wR2 = 0.1953
R indices (all data)	R1 = 0.1162, wR2 = 0.2360
largest diff.peak and hole (eÅ^{-3})	10.493 and −7.549 eÅ^{-3}

Platon/SQUEEZE[41] was used to determine the void volume in each of the three structures, approximating to an additional 50 hydrogen-bonded water molecules per unit cell. The void volumes present were 1899 Å^3 for La, 2016 Å^3 for Nd, and 2054 Å^3 for Eu, representing 12.1, 12.6, and 24.5% of the unit cell volumes, respectively.

Comments on the Crystal Structures. It is typical to observe peaks adjacent to the W atoms in POMs, as seen in these structures.[42−46] The large residual peaks and high R_{int} values

(41) Sluis, P.; Spek, A. *Acta Crystallogr., Sect. A* **1990**, *A46*, 194−206.
(42) Ortega, F.; Pope, M. T.; Evans, J. H. G. *Inorg. Chem.* **1997**, *36*, 2166−2169.
(43) Sazani, G.; Dickman, M. H.; Pope, M. T. *Inorg. Chem.* **2000**, *39*, 939−943.
(44) Wasserman, K.; Lunck, H. J.; Palm, R.; Fuchs, J.; Steinfeldt, N.; Stoesser, R.; Pope, M. T. *Inorg. Chem.* **1996**, *35*, 3273−3279.
(45) Xin, F.; Pope, M. F. *Inorg. Chem.* **1996**, *35*, 5693−5695.

Table 3. Selected Bond Lengths and Angles for $[Ln(\alpha_1\text{-}P_2W_{17}O_{61})_2]^{17-}$

La1−O9 2.480(11)	Nd−O2N 2.467(4)	Eu−O11E 2.402 (25)	Eu−O22E 2.397 (15)
La1−O21 2.471(5)	Nd−O6N 2.445(8)	Eu−O2E 2.351 (35)	Eu−O26E 2.365 (18)
La1−O39 2.506(7)	Nd−O11N 2.378(11)	Eu−O9E 2.402 (47)	Eu−O31E 2.356 (56)
La1−O61 2.445(10)	Nd−O9N 2.475(10)	Eu−O6E 2.411 (36)	Eu−O27E 2.378 (26)

observed in the Eu and Nd analogues may also be due to the decomposition of the crystals as the data is being collected.

Results

1. Stability Constant Determination. The conditional stability constants, log K_{1cond} (eq 24) and log K_{2cond} (eq 25), for Ln complexes of $(\alpha_1\text{-}P_2W_{17}O_{61})$,$^{10-}$ shown in Table 3, were determined using ^{31}P NMR spectroscopy. An advantage to this ^{31}P NMR method is that, in addition to a direct determination of the concentrations, the exact speciation in solution can be monitored. Understanding the speciation is critical, especially in the case of the $(\alpha_1\text{-}P_2W_{17}O_{61})^{10-}$, because this POM is unstable and easily isomerizes to the $(\alpha_2\text{-}P_2W_{17}O_{61})^{10-}$ isomer and, at low pH, decomposes to the $(\alpha\text{-}P_2W_{18}O_{62})^{6-}$ Wells−Dawson POM.[47,48] The chemical shifts of the $(\alpha_1\text{-}P_2W_{17}O_{61})^{10-}$ and $(\alpha_2\text{-}P_2W_{17}O_{61})^{10-}$ ligands and their lanthanide complexes are quite different; therefore, we can easily verify that only the $(\alpha_1\text{-}P_2W_{17}O_{61})^{10-}$ species and the Ln(III) complexes are in solution. Figure 1 shows sample ^{31}P experiments to determine K_{1cond} and K_{2cond}.

$$Ln + (\alpha_1\text{-}P_2W_{17}O_{61})^{10-} \rightleftharpoons (H_2O)_4Ln\,(\alpha_1\text{-}P_2W_{17}O_{61})^{7-} \qquad K_{1cond} \quad (24)$$

$$(H_2O)_4Ln\,(\alpha_1\text{-}P_2W_{17}O_{61})^{7-} + (\alpha_1\text{-}P_2W_{17}O_{61})^{10-} \rightleftharpoons Ln\,(\alpha_1\text{-}P_2W_{17}O_{61})_2^{14-} \qquad K_{2cond} \quad (25)$$

The conditional K_{1cond} was determined using a competitive method with EDTA as the competitive ligand, according to eq 1. From our previous work[39,40] and that of others,[23] it was clear that, at 1:1 stoichiometry, only the 1:1 complex existed in solution, and thus, the 1:2 species was not considered in this K_{1cond} determination. Indeed, the ^{31}P NMR for the K_{1cond} experiment showed no evidence of the 1:2 complex nor any other complex involving the $(\alpha_1\text{-}P_2W_{17}O_{61})^{10-}$ ligand.

The ligand EDTA met the following conditions for a competitive ligand: (1) Lanthanide EDTA complexes are well characterized and only form a 1:1 complex, whose thermodynamic formation constant is known. (2) The value of the formation constant of LnEDTA complexes are compatible with the formation constant of $[\alpha_1\text{-}P_2W_{17}O_{61}]^{10-}$ with lanthanide(III) ions at the pH (4.75) chosen for the experiments (about log $K \approx 10$). Strong complexation of EDTA with Eu(III) is well-known, and the thermodynamic binding constant is about $10^{17}-10^{19}$. Lowering the pH results in a competition between protons and EDTA, and the conditional equilibrium constant (K'_{cond}) may be lowered to match the conditional equilibrium constant for Ln/$(\alpha_1\text{-}P_2W_{17}O_{61})^{10-}$. At pH 2−6, the conditional formation constant for EuEDTA changes from 3.91 to 12.76.[49] Therefore, by varying the solution pH, EDTA can be used as a competitive ligand for the measurements of formation constants of a variety of lanthanide complexes that have different binding strengths.

At stoichiometries > 2, an equilibrium can be set up between the 1:1 and 1:2 species that can be examined by ^{31}P NMR spectroscopy. Thus, when the approach described in the Experimental section is used, the conditional K_{2cond} can be determined from the ^{31}P NMR. K_{2cond} is highly dependent on the countercation (Table 3) and on the concentration of the counterion. Measurements of K_{2cond} for the Eu/$[\alpha_1\text{-}P_2W_{17}O_{61}]^{10-}$ complex as a function of Li^+ ions show that the log K_{2cond} value decreases significantly as the Li^+ concentration increases (Supporting Information). For example, log K_{2cond} ranges from 2.177 ± 0.003 at 0.02 M Li^+ to 0.779 ± 0.024 at 1.0 M Li^+ (Supporting Information). We did not measure the protonation constants of the $[\alpha_1\text{-}P_2W_{17}O_{61}]^{10-}$ ligand and, thus, cannot calculate the thermodynamic stability constants. However, this study allows a valuable comparison of the conditional stability constants across the lanthanide series.

The only other studies of the stability constants of Ln(III) complexes of the $\alpha_1\text{-}P_2W_{17}O_{61}{}^{10-}$ isomer were reported by Ciabrini and Contant for the Ce(III) analogues.[50] Our data (K_1,K_2, log K_1/log K_2) are consistent with the conditional stability constants reported in that study for the Ce(III) complexes of the $\alpha_1\text{-}P_2W_{17}O_{61}{}^{10-}$ isomer (1 M $LiNO_3$; log K_1 = 6.6; log K_2 = 1.5; log K_1/log K_2 = 4.4) using spectrophotometric and potentiometric techniques. It is expected that the K_1 and K_2 values, measured in 1.0 M Li^+ would be lower than ours that are measured in 0.5 M Li^+ buffer.

2. Synthesis and Crystal Structure. Treatment of $(\alpha_1\text{-}P_2W_{17}O_{61})^{10-}$ with $LnCl_3$ in a lithium buffer resulted in the precipitation of a white solid that, upon crystallization, gave crystals with the 1:2 Ln/$(\alpha_1\text{-}P_2W_{17}O_{61})^{10-}$ (Ln = La, Nd, Eu, Er) formulation. The formulation of $K_{14}(H_3O)_3[Ln(\alpha_1\text{-}P_2W_{17}O_{61})_2]\cdot xH_2O$ for the analogues was confirmed by an elemental analysis of the crystals.

Synthesis, crystallization, and X-ray crystallographic analyses of the 1:2 Ln/$(\alpha_1\text{-}P_2W_{17}O_{61})^{10-}$ (Ln = La, Nd, Eu, Er) species were compromised by the lack of stability, as expected by the low stability constants. Indeed, crystal decomposition hindered the X-ray diffraction analysis. All of the crystals (La through Er) showed the 1:2 formulation and, moreover, confirmed unambiguously that the

(46) Zhang, X. Y.; O'Connor, C. J.; Jameson, G. B.; Pope, M. T. *Inorg. Chem.* **1996**, *35*, 30−34.
(47) Contant, R.; Ciabrini, J.-P. *J. Chem. Res., Synop.* **1977**, *222*; *J. Chem. Res., Miniprint* **1977**, 2601−2617.
(48) Contant, R.; Teze, A. *Inorg. Chem.* **1985**, *24*, 4610−4618.
(49) Martell, A. E.; Smith, R. M. *Critical Stability Constants*; Plenum Press: New York, 1974; Vol. 1.
(50) Ciabrini, J.-P.; Contant, R. *J. Chem. Res., Miniprint* **1993**, 2720−2744.

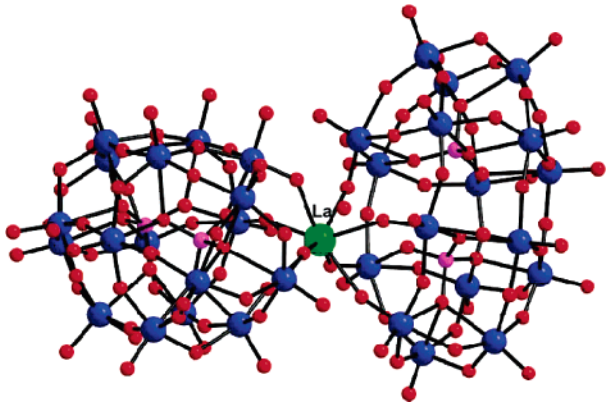

Figure 2. Ball-and-stick representation of the 1:2 $[La(\alpha_1\text{-}P_2W_{17}O_{61})_2]^{17-}$ (green = La; blue = W; red = O; pink = P).

(α_1-$P_2W_{17}O_{61})^{10-}$ POM maintained its integrity. Figure 2 shows a ball-and-stick diagram of the La(III) analogue that gave the highest quality data. Figure S1 in the Supporting Information shows representations of the La and Eu analogues with 50% ellipsoids.

The Yb and Lu 1:2 Ln/(α_1-$P_2W_{17}O_{61})^{10-}$ analogues could not be isolated. Crystals that were isolated after about a week from the prep designed to give the 1:2 Lu/(α_1-$P_2W_{17}O_{61})^{10-}$ analogue were determined by X-ray crystallography to be the 1:2 Lu/(α_2-$P_2W_{17}O_{61})^{10-}$ complex. Obtaining this α_2 product is consistent with the lack of stability of the 1:2 Lu/(α_1-$P_2W_{17}O_{61})^{10-}$ complex and isomerization to the (α_2-$P_2W_{17}O_{61})^{10-}$ derivative.

The relative orientation of the two α_1 lobes can be described by two angles, shown in Figure 3. The first angle describes the "rotation" of the units relative to each other. This angle can be assessed by constructing a plane through both phosphorus atoms and the lanthanide atom in each unit and then calculating the angle between these planes. This angle does not show significant variation, changing from 111°, 108°, and 112° for La(III), Nd(III), and Eu(III), respectively. The second angle, which shows significant variation, can be described as an "opening up" of the units. This angle is assessed by constructing planes through both phosphorus atoms, the apical phosphorus oxygen atoms, and a bridging oxygen in the cap region. This angle changes from 64.5°, 77.2°, and 81.6° for La(III), Nd(III), and Eu(III), respectively, reflecting the spreading apart of the POM lobes.

The X-ray crystallography data reveal the source of the instability of the 1:2 complex. The Ln(III) center is bound, in a square antiprismatic coordination geometry, to two (α_1-$P_2W_{17}O_{61})^{10-}$ units. As expected, the Ln−O bond lengths decrease as the Ln series is traversed. As a response to the decreasing bond lengths, the two (α_1-$P_2W_{17}O_{61})^{10-}$ moieties spread apart, as seen from the increase in the acute angle, which represents the spreading apart of the two (α_1-$P_2W_{17}O_{61})^{10-}$ moieties (Figure 3). The acute angle results in closer contact of the POM lobes, resulting in steric encumbrance.

3. Multinuclear NMR Spectroscopy. The ^{31}P NMR and ^{183}W spectra of the 1:2 species can only be obtained in D_2O, that is high in salt content, using either KCl or CsCl. When crystals of $[Ln(\alpha_1\text{-}P_2W_{17}O_{61})_2]^{17-}$ are dissolved in solutions of Li^+, only the 1:1 species and ligand are observed, vide infra. The ^{31}P NMR spectra for the Eu(III) analogue and the La(III) and Nd(III) analogues (>0.1 M KCl) are shown in Figures 4 and S2 (Supporting Information), respectively. Table S3 in the Supporting Information shows the ^{31}P NMR chemical shifts for the La, Nd, and Eu analogues. The ^{31}P NMR spectrum for the Eu species, perhaps because of the shift reagent properties of Eu(III), shows two sets of peaks, whereas the peaks are broadened and slightly unsymmetrical for the La and Nd analogues. Thus, we speculate that there are two species with the formulation of 1:2 in solution. The major species for the Eu(III) analogue shows two P resonances, consistent with the equivalence of each (α_1-$P_2W_{17}O_{61})^{10-}$ unit. This species may represent a species, with C_i point group symmetry, where the (α_1-$P_2W_{17}O_{61})^{10-}$ units are rotated to be "trans" to each other. The minor species appears to show a "doublet" in the downfield region, possibly consistent with the C_1 symmetry of the 1:2 species, as isolated in the crystal structure. Preliminary excitation spectroscopy (0.5 M KCl) shows one type of Eu(III) environment. Luminescence lifetime measurements[51−53] taken in 0.5 M KCl in D_2O and H_2O for the Eu(III) analogue show $q = 0.34$, suggesting that no water molecules are bound to the Eu(III) center, consistent with the 1:2 formulation.

The ^{183}W NMR spectrum for the La(III) analogue, Figure S3 in the Supporting Information, shows 16 peaks (2 overlap at −215 ppm) and is consistent with the major species, as observed in the ^{31}P NMR spectrum, representing a species where the two (α_1-$P_2W_{17}O_{61})^{10-}$ units are equivalent. These resonances are at different chemical shifts from those of the lacunary and 1:1 species. The resonances for the minor species are likely not observed as described below. Although ^{183}W NMR spectroscopy is very sensitive, the low abundance of ^{183}W (14%) renders the spectra difficult to obtain for species of low symmetry. The (α_1-$P_2W_{17}O_{61})^{10-}$ POM ligand possesses C_1 point group symmetry; thus, all 17 W atoms are not equivalent. For the major 1:2 species where, we postulate, the two (α_1-$P_2W_{17}O_{61})^{10-}$ lobes are equivalent, 17 lines would be observed. For a minor species where the two (α_1-$P_2W_{17}O_{61})^{10-}$ lobes are not equivalent, 34 resonances would be observed. Given the low concentration of this species, its lack of symmetry, and the inherent low abundance of the ^{183}W nucleus, it is highly likely that the 34 resonances are buried in the noise of the spectrum. The multinuclear NMR data and the luminescence spectroscopy suggest that there may be two types of 1:2 Ln/(α_1-$P_2W_{17}O_{61})^{10-}$ species in solution, and it is very likely that they are conformers and differ only in the disposition of the (α_1-$P_2W_{17}O_{61})^{10-}$ units relative to each other. Further experiments are warranted to investigate the temperature dependence of the putative conformations. It is very likely, however, that the determination of K_{2cond} is on a mixture of conformers, with the 1:2 formulation.

(51) Horrocks, W. D., Jr.; Sudnick, D. R. *J. Am. Chem. Soc.* **1979**, *101*, 334−340.
(52) Horrocks, W. D., Jr.; Sudnick, D. R. *Science* **1979**, *206*, 1194−1196.
(53) Horrocks, W. D., Jr. *Methods Enzymol.* **1993**, *226*, 495−538.

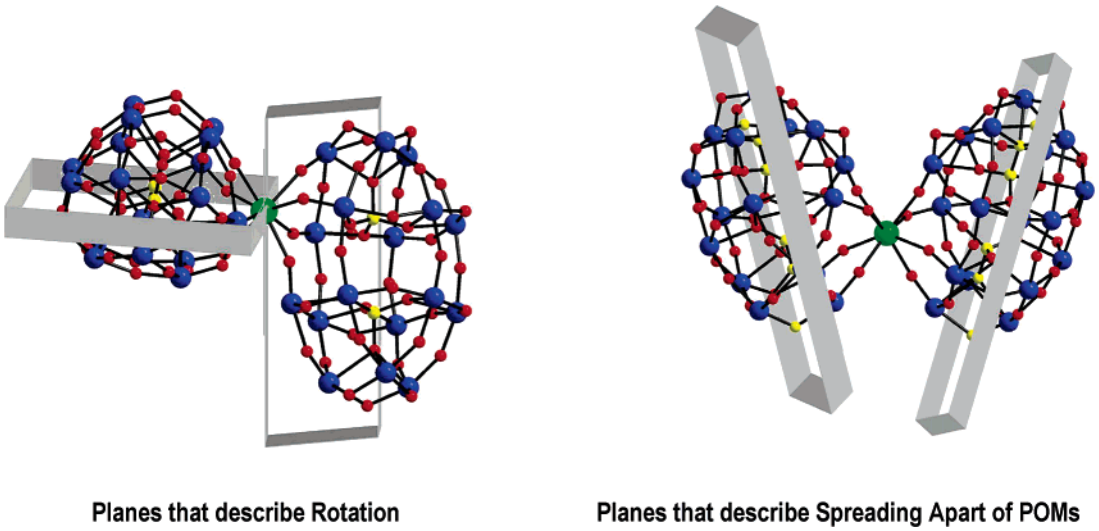

Figure 3. Display of angles between two $(\alpha_1\text{-}P_2W_{17}O_{61})^{10-}$ units in $[Ln(\alpha_1\text{-}P_2W_{17}O_{61})_2]^{17-}$.

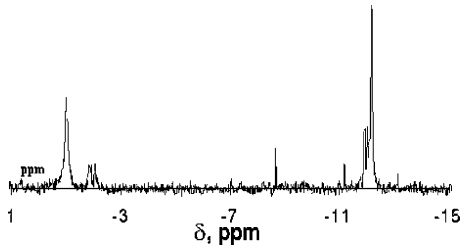

Figure 4. ^{31}P NMR Data for $[Eu(\alpha_1\text{-}P_2W_{17}O_{61})_2]^{17-}$ dissolved in 0.125 M KCl (30% D_2O).

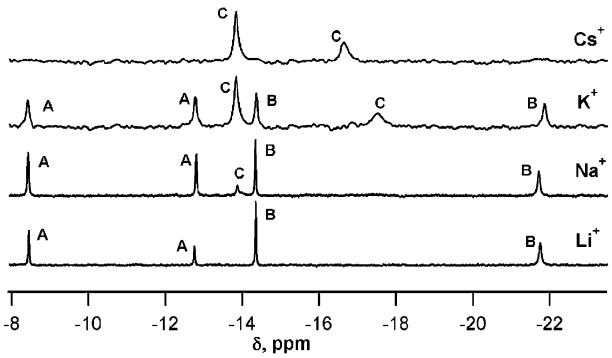

Figure 5. Speciation dependence of 0.01 mmol of $[Nd(\alpha_1\text{-}P_2W_{17}O_{61})_2]^{17-}$ on the countercation (0.04 M) in water monitored by ^{31}P NMR spectroscopy. (A) Ligand $[\alpha_1\text{-}P_2W_{17}O_{61}]^{10-}$. (B) 1:1 $[Nd(\alpha_1\text{-}P_2W_{17}O_{61})]^{7-}$. (C) 1:2 $[Nd(\alpha_1\text{-}P_2W_{17}O_{61})_2]^{17-}$.

A dependence on the countercation was observed and is consistent with the stability constant measurements. Crystals of $[Nd(\alpha_1\text{-}P_2W_{17}O_{61})_2]^{17-}$ dissolved in an aqueous buffer clearly show the speciation dependence on the counterion (Figure 5). The 1:2 complex is stabilized by Cs^+ (0.04 M); an equilibrium between the 1:2 and 1:1 complexes and the $(\alpha_1\text{-}P_2W_{17}O_{61})^{10-}$ ligand is observed in 0.04 M K^+ and Na^+, and only the 1:1 complex and the $(\alpha_1\text{-}P_2W_{17}O_{61})^{10-}$ ligand are observed in 0.04 M Li^+ buffer.

Titration of $(\alpha_1\text{-}P_2W_{17}O_{61})^{10-}$ into a 1:1 Eu/$(\alpha_1\text{-}P_2W_{17}O_{61})^{10-}$ solution in a dilute KCl medium shows the buildup of the 1:2 species (Figure S4 in the Supporting Information). At a 1:2.5 Eu(III)/$(\alpha_1\text{-}P_2W_{17}O_{61})^{10-}$ stoichiometry, it is clear that there are significant amounts of the 1:1 species and the ligand as well as the 1:2 species.

Discussion

The 1:1 Ln/$(\alpha_1\text{-}P_2W_{17}O_{61})^{10-}$ species has recently been documented both in solution and in the solid state. The 1:1 Ce(III)/$(\alpha_1\text{-}P_2W_{17}O_{61})^{10-}$ species is a "2:2" dimer in the solid state wherein the Ce(III) is nine coordinate, bound to four oxygen atoms of the lacunary $(\alpha_1\text{-}P_2W_{17}O_{61})^{10-}$ POM, four water molecules, and to a terminal W−O of an adjacent $(\alpha_1\text{-}P_2W_{17}O_{61})^{10-}$ moiety.[23] The molecule decomposes into a 1:1 monomer in aqueous solution. We described the 1:1 formulation across the lanthanide series by luminescence measurements and complexometric titrations[39] and found a monomer in the solid state for the Lu(III) analogue.[40] Contant described the formation of the 1:1 and 1:2 Ce(III) species in aqueous solution.[50] Our data (K_{1cond}, K_{2cond}, log K_{1cond}/log K_{2cond}) are consistent with the conditional stability constants reported in that study.

The increase of K_{1cond}, as the lanthanide series is traversed, is consistent with our synthetic observations that isolation of the 1:1 Ln/$(\alpha_1\text{-}P_2W_{17}O_{61})^{10-}$ species is more facile for the later lanthanides than for the early to mid lanthanides.[39] Our conditional stability constant data support the notion that the high basicity of the α_1 vacancy requires high charge/size cations for stabilization. The high basicity of the α_1 defect has been ascribed to the orientation of the PO_4^{3-} tetrahedron within the cavity of the W−O framework, positioning a basic oxygen atom near the α_1 site. This basic oxygen is bound to one P atom and one W atom, compared to the oxygen atoms of the PO_4^{3-} tetrahedron near the α_2 site that are bound to one P atom and two W atoms, Figure 6.[50] It is also likely that the later, heavier lanthanides with shorter Ln−O bond lengths will be suitably accommodated in the α_1 defect site to stabilize the resulting 1:1 Ln$(\alpha_1\text{-}P_2W_{17}O_{61})^{10-}$ species.

The 1:2 Ln/$(\alpha_1\text{-}P_2W_{17}O_{61})^{10-}$ complexes have been more elusive. Contant notes that these species form only in high sodium content and are unstable.[50] In an early publication,

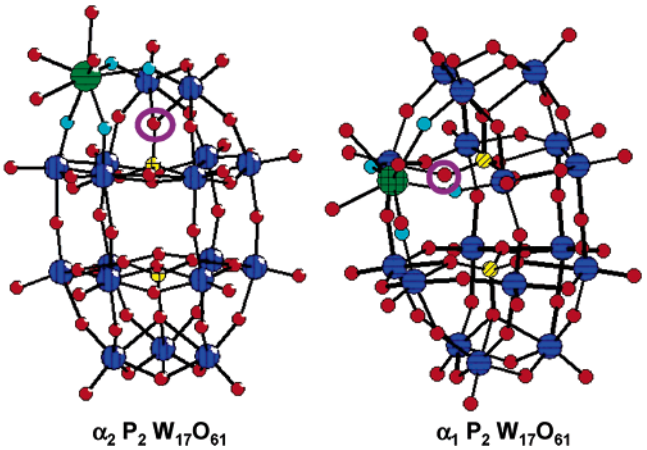

Figure 6. General representations of $[Ln(III)(\alpha_2\text{-}P_2W_{17}O_{61})]^{7-}$ and $[Ln(III)(\alpha_1\text{-}P_2W_{17}O_{61})]^{7-}$ complexes showing the position and composition of the defect sites. The defect site of the α_1-$P_2W_{17}O_{61}^{10-}$ is considered highly basic primarily because of the oxygen atom, circled in violet, that is bound to one P atom and one W atom. This site appears to require high charge/size ions for stability.

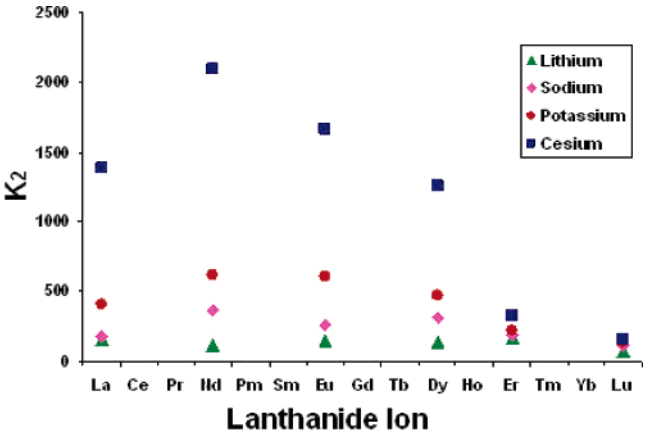

Figure 7. Graph of K_2 for the formation of $[Ln(\alpha_1\text{-}P_2W_{17}O_{61})_2]^{17-}$ as a function of the lanthanide ion and countercation. See text and Table 3 for conditions.

we noted that, upon crystallization of solids that were prepared with 1:2 La/$(\alpha_1$-$P_2W_{17}O_{61})^{10-}$ stoichiometry, we observed small, broad (often multiplet) peaks appearing close to the peaks that represent the 1:1 compound. We did not see such resonances in the ^{31}P NMR spectra for the later lanthanides. We postulated that these were the 1:2 species.[39] In this study, we have isolated 1:2 Ln/$(\alpha_1$-$P_2W_{17}O_{61})^{10-}$ species for the early−mid lanthanides. The stability constant data (K_{2cond}), solution speciation data, and crystallography suggest the rationale for their formation and high instability.

The conditional log K_{2cond} constants for Ln complexes of $(\alpha_1$-$P_2W_{17}O_{61})^{10-}$ are much lower than the log K_{1cond} constants. The 1:2 complexes are quite unstable in the solid state, decomposing easily even under low temperatures, as experienced during crystal structure data collection. The K_{2cond} constants are dependent on the countercation (Li^+, Na^+, K^+, and Cs^+) and on the lanthanide ionic radius as well. The maximum K_2 occurs at Nd(III) (Figure 7); this likely reflects two components. The first is that the charge-to-size ratio of the Ln(III) ion impacts the electrostatic affinity for the α_1 defect. This is reflected in the later lanthanides having a higher affinity for the α_1 site. The second component to be considered is the severe steric strain imposed on the 1:2 complex as a result of the decrease of bond lengths as the Ln series is traversed. These competing forces apparently place the mid lanthanides at the highest K_2 value. The steric issues are particularly important in the case of the later lanthanides. The Yb and Lu compounds cannot be isolated. A preparation designed to produce the 1:2 Lu(III)/$(\alpha_1$-$P_2W_{17}O_{61})^{10-}$ species lead to crystals of the 1:2 Lu(III)/$(\alpha_2$-$P_2W_{17}O_{61})^{10-}$ species, confirming the lack of stability of the 1:2 Lu(III)/$(\alpha_1$-$P_2W_{17}O_{61})^{10-}$ complex.

The concept that the countercation influences the equilibria was discussed by Ciabrini and Contant, who report that the 1:2 Ce(III) species could be formed only in high Na^+ content and was unstable.[50] The effects of counterions in the formation of 1:2 Th/$(\alpha_2$-$P_2W_{17}O_{61})^{10-}$ was put forth by Kirby and Baker; they postulated that the K^+ ion supports the formation of the "syn" complex.[54] We and others have observed that Cs^+ promotes the 1:2 formation of $Eu(PW_{11}O_{39})_2^{11-}$ and $K(SiW_{11}O_{39})_2$.[15−55,56] The stabilization of the 1:2 Ln/$(\alpha_1$-$P_2W_{17}O_{61})^{10-}$ species by K^+ and Cs^+ is evident from this study. This effect of Cs^+ appears to be quite general. It is likely that the oligomerization of the Ln POMs is due to the ion pairing of the larger countercations to the POM surface, possibly anchoring the POMs close to the Ln(III) center, positioning the POM for optimal binding. In studies by Hill and Weinstock the larger and less extensively solvated alkali-metal cations form smaller (more intimate) association complexes with the $\{X^{n+}VW_{11}O_{40}\}^{(9-n)-}$ [X = P(V), Si(IV), Al(III)] family of POMs.[57,58] In a similar fashion, we suspect that the Cs^+ ions and, to an extent, the K^+ ions are binding to surface sites of POMs and thus stabilize the 1:2 structures in solution.

Another factor that may play into the countercation stability is the affinity for the $(\alpha_1$-$P_2W_{17}O_{61})^{10-}$ POM for Li^+. Contant revealed that the log K value for the Li^+ ion complex of the $(\alpha_1$-$P_2W_{17}O_{61})^{10-}$ species was > 3.7, whereas for Na^+ and K^+, the log K values were significantly lower, ca. 0.7. The log K values for Li^+ and Na^+ complexes of $(\alpha_2$-$P_2W_{17}O_{61})^{10-}$ were closer.[59] This suggests that Li^+ competes very effectively for the $(\alpha_1$-$P_2W_{17}O_{61})^{10-}$ POM and, perhaps, as suggested by Ciabrini and Contant, in the defect site. Indeed, this notion is consistent with our ^{31}P NMR work (Figure 5) where the 1:2 Nd/$(\alpha_1$-$P_2W_{17}O_{61})^{10-}$ decomposes completely into the 1:1 species and ligand when dissolved in a buffer prepared with Li^+. Na^+, K^+, and Cs^+ promote the 1:2 formation, and Cs^+ exclusively promotes the formation of the 1:2 species.

A comparison with the lanthanide complexes of α_2-$P_2W_{17}O_{61}^{10-}$ is very interesting and informative. A few studies report stability constants (conditional and thermo-

(54) Kirby, J. F.; Baker, L. C. W. *Inorg. Chem.* **1998**, *37*, 5537−5545.
(55) Zhang, C.; Howell, R. C.; Scotland, K. B.; Perez, F. G.; Todaro, L.; Francesconi, L. C. *Inorg. Chem.* **2004**, *43*, 7691−7701.
(56) Laronze, N.; Marrot, J.; Herve, G. *Inorg. Chem.* **2003**, *42*, 5857−5862.
(57) Grigoriev, V. A.; Hill, C. L.; Weinstock, I. A. *J. Am. Chem. Soc.* **2000,** *122*, 3544−3545.
(58) Grigoriev, V. A.; Cheng, D.; Hill, C. L.; Weinstock, I. A. *J. Am. Chem. Soc.* **2001**, *123*, 5292−5307.
(59) Contant, R.; Ciabrini, J.-P. *J. Chem. Res., Miniprint* **1982**, 641−660.

dynamic) for Ln complexes of α_2-$P_2W_{17}O_{61}^{10-}$. These studies suggest that K_1 and K_2 remain constant over the series[31,60,61] or increase slightly from La to Eu and remain constant from the mid to late lanthanides.[62] Generally, the thermodynamic log K_1 and log K_2 are on the order of 10.35−12.7 and 6−8.1, respectively, and log K_1/log K_2 are ca. 1.30−1.70. Ciabrini reported conditional constants for Ce(III) α_2-$P_2W_{17}O_{61}^{10-}$ (log K_1 = 8.8, log K_2 = 6.0, log K_1/log K_2 = 1.47).[50] Our own data on lanthanide complexes of α_2-$P_2W_{17}O_{61}$,$^{10-}$ using NMR competition methods and luminescence titrations, are consistent with these studies. We find that, for Ln complexes of α_2-$P_2W_{17}O_{61}$,$^{10-}$ log K_1 is relatively constant for lanthanides spanning the Ln series (La−Lu) at ca. 11.3−12.5 and log K_2 is also constant, ranging from 5.8 to 6.6 and the log K_1/log K_2 ratio = 1.95−2.00.[63]

In contrast, the log K_{1cond}/log K_{2cond} ratio for the lanthanide α_1-$P_2W_{17}O_{61}^{10-}$ series is 3.65 for La(III), increasing to 6.67 for Lu(III). These are even slightly underestimated because the buffer conditions used were 0.5 M Li^+ for K_{1cond} and 0.02 M Li^+ for K_{2cond} determinations. However, the striking differences in K_1 and K_2 for Ln complexes of α_1-$P_2W_{17}O_{61}^{10-}$ compared to those found for the studies of Ln complexes of α_2-$P_2W_{17}O_{61}^{10-}$ are the reasons that the 1:1 Ln/α_1-$P_2W_{17}O_{61}^{10-}$ complexes can be isolated, especially for the later lanthanides. In contrast, mixtures of the 1:1 and 1:2 species are often isolated for Ln complexes of α_2-$P_2W_{17}O_{61}^{10-}$ and monovacant Keggin complexes. Moreover, the demonstrated effect of the countercations suggests that the syntheses of the 1:1 or the 1:2 Ln/α_1-$P_2W_{17}O_{61}^{10-}$ complexes can be tuned by a judicious choice of countercation. We are using these important principals to design synthetic strategies to produce organic soluble 1:1 Ln/α_1-$P_2W_{17}O_{61}^{10-}$ complexes that can be further reacted with a variety of organic ligands, including sensitizing groups, to form hybrid inorganic−organic lanthanide POMs.

Conclusion

The stabilization of the 1:1 Ln/(α_1-$P_2W_{17}O_{61}$)$^{10-}$ complexes with respect to the 1:2 complexes is due to the high conditional stability constant, K_{1cond}, and the very low K_{2cond}. The low K_{2cond} is derived from the severe steric strain due to the proximity of the (α_1-$P_2W_{17}O_{61}$)$^{10-}$ lobes to each other as the Ln−O bond lengths decrease across the lanthanide series. Countercations play a significant role in tuning the K_{2cond} and, thus, the stabilization of the 1:2 complex. These principles can be used for the design of syntheses to produce aqueous and organic soluble 1:1 Ln/α_1-$P_2W_{17}O_{61}^{10-}$ complexes that can be further reacted with a variety of organic ligands.

Acknowledgment. We acknowledge the following sources of support for this research: NSF Grant CHE 0414218, NIH-S06 GM60654 (SCORE) (L.C.F.); the Faculty Research Award Program of the City University of New York, Eugene Lang Faculty Development Award (L.C.F.); the Gertrude Elion Fellowship and Rose Kefar Rose Dissertation Award (C.Z.); and NSF Grant MRI0116244 for the purchase of an X-ray diffractometer (L.C.F.). Research Infrastructure at Hunter College is partially supported by NIH Research Centers in Minority Institutions (Grant RR03037-08).

Supporting Information Available: The Supporting Information includes sample calculations for K_{1cond} and K_{2cond} and K_{2cond} as a function of [Li^+]. Also available are Table S2, crystal data in CIF format, a structure refinement table for $K_{14}(H_3O)_3$[Ln(α_1-$P_2W_{17}O_{61})_2$]·$n$$H_2O$ (Ln = Eu, Nd), and Figure S1a,b, representations as 50% ellipsoids of [Eu(α-1-$P_2W_{17}O_{61})_2$]$^{17-}$ and [La(α_1-$P_2W_{17}O_{61})_2$].$^{17-}$ Multinuclear NMR data, Table S3, and Figures S2, S3, and S4 are also available. This material is available free of charge via the Internet at http://pubs.acs.org.

IC050103O

(60) Lu, Y.-W.; Keita, B.; Nadjo, L. *Polyhedron* **2004**, *23*, 1579−1586.
(61) Bion, L.; Mercier, F.; Decambox, P.; Moisy, P. *Radiochim. Acta* **1999**, 161−166.
(62) Van Pelt, C. E.; Crooks, W. J., III; Choppin, G. R. *Inorg. Chim. Acta* **2003**, *346*, 215−222.
(63) Zhang, C.; Feng, X.; Howell, R. C.; Luo, Q.; McGregor, D.; Bensaid, L.; Todaro, L.; Francesconi, L. C. *Manuscript in preparation*, 2005.